# Nanoporous germanium prepared by a mechanochemical reaction with enhanced lithium storage properties

Xianyu Liu,*[a, d] Qianliang Zhang,[b] Yansong Zhu,[b] Shengjie Xu,[c] Jia Zhang,[c] Yanping Zheng,[a] Lei Zhang,[a] Mingguang Ma,[a] Honghong Rao[a] and Zheng Liu*[a]

[a] School of Chemical Engineering, Institute of Urban Ecology and Environment, Nanomaterials Laboratory, Lanzhou City University, Lanzhou, Gansu 730070, The People's Republic of China.

[b] Key Laboratory of Colloid and Interface Chemistry, Ministry of Education, School of Chemistry and Chemical Engineering, and State Key Laboratory of Crystal Materials, Shandong University, Jinan, Shandong 250100, The People's Republic of China.

[c] School of Applied Chemical Engineering, Lanzhou Petrochemical University of Vocational Technology, Lanzhou, Gansu 730060, The People's Republic of China.

[d] Hefei National Laboratory for Physical Science at the Microscale, Department of Applied Chemistry, University of Science and Technology of China, Hefei, 230026, The People's Republic of China.

Corresponding Author

Xianyu Liu, E-mail: xyliu15@mail.ustc.edu.cn

Zheng Liu, E-mail: liuzh@lzcu.edu.cn

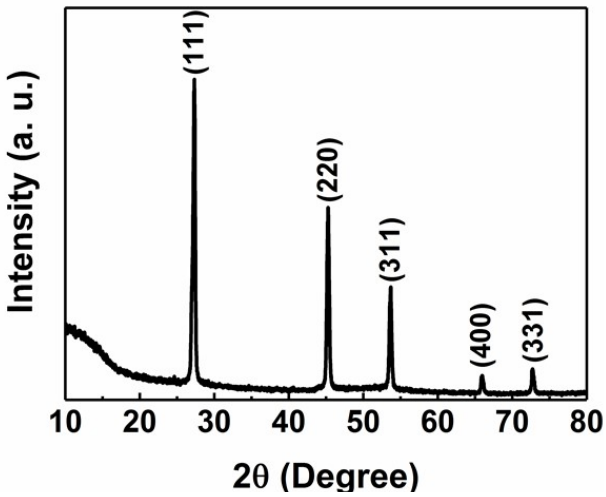


**Figure S1.** XRD patterns of the nanoporous A-Ge materials.

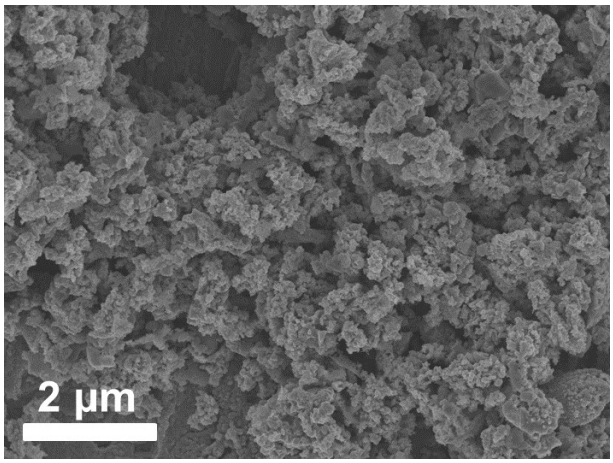


**Figure S2.** SEM image of the nanoporous A-Ge materials.

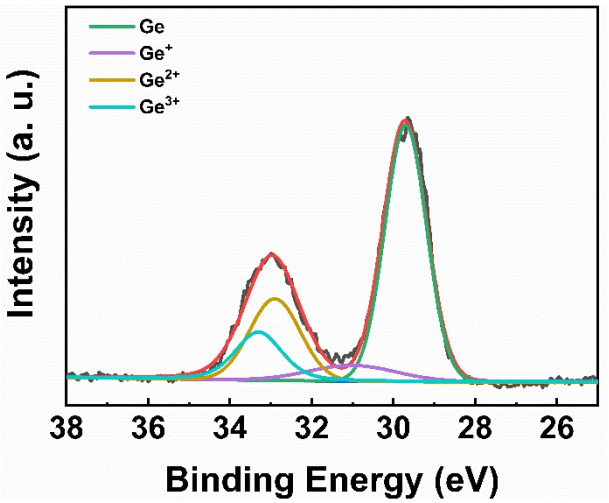


**Figure S3.** XPS spectra of Ge 3d of nanoporous A-Ge materials.

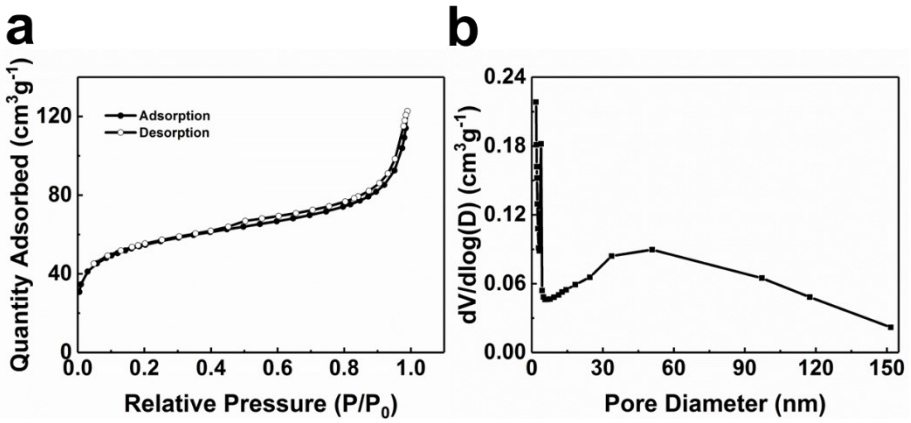


**Figure S4.** (a) $N_2$ adsorption-desorption isotherms and (b) the pore-size distribution calculated from the desorption branch of the nanoporous A-Ge materials.

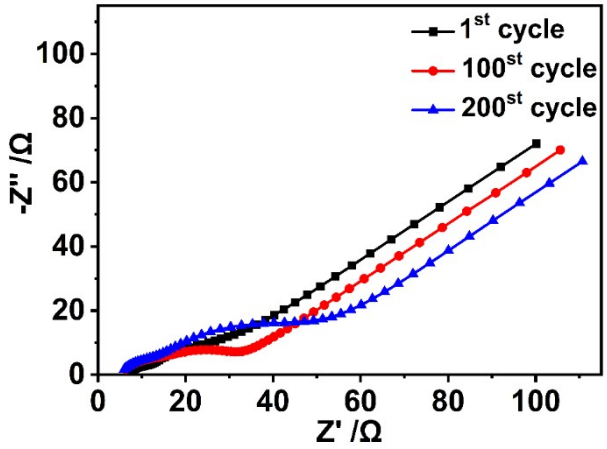


**Figure S5.** Electrochemical impedance spectra (EIS) of Z-Ge materials.

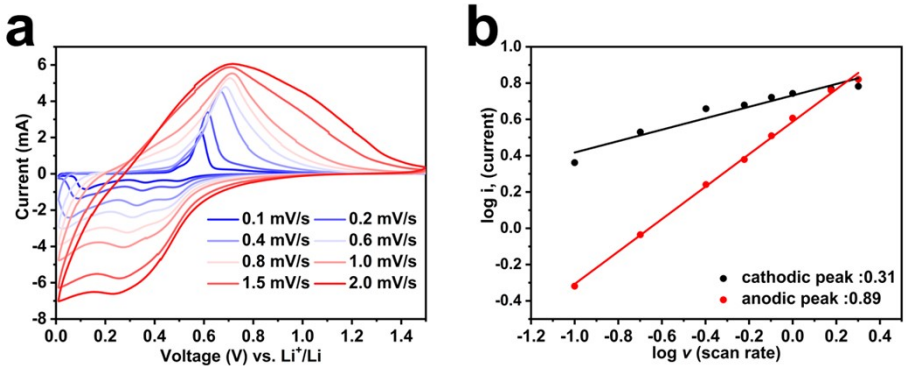


**Figure S6. (**a) Curves at various scan rates from 0.1 to 2 mV $s^{-1}$. (b) log (i) versus log (v) plots and b value for the slope.

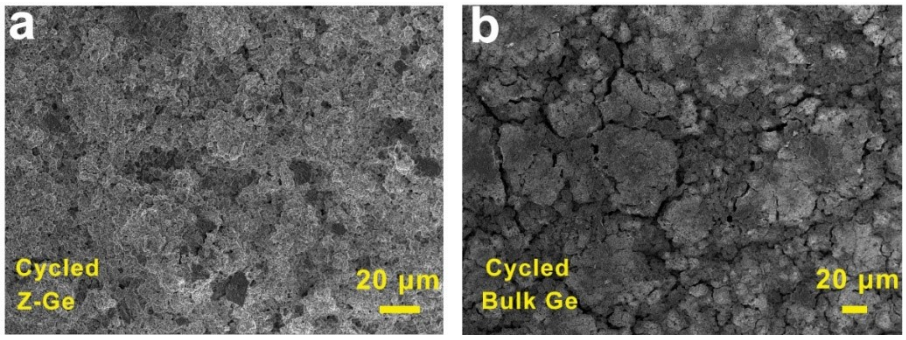


**Figure S7.** FESEM images of (a) Z-Ge and (b) bulk Ge electrodes after 100 cycles.

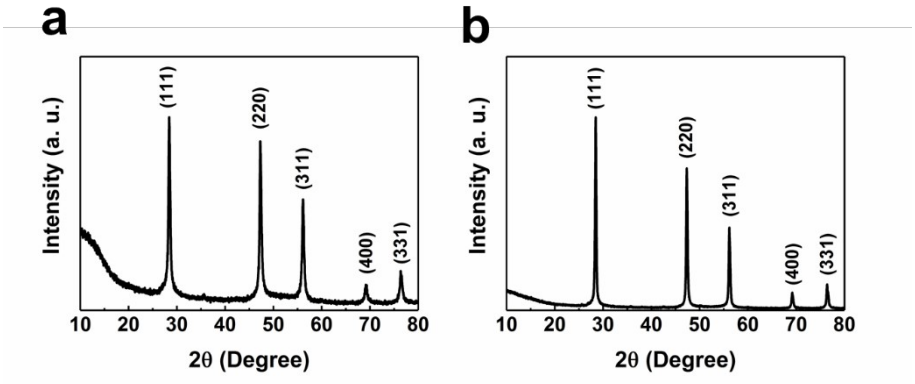


**Figure S8.** XRD patterns of the nanoporous Z-Si (a) and A-Si (b) materials.

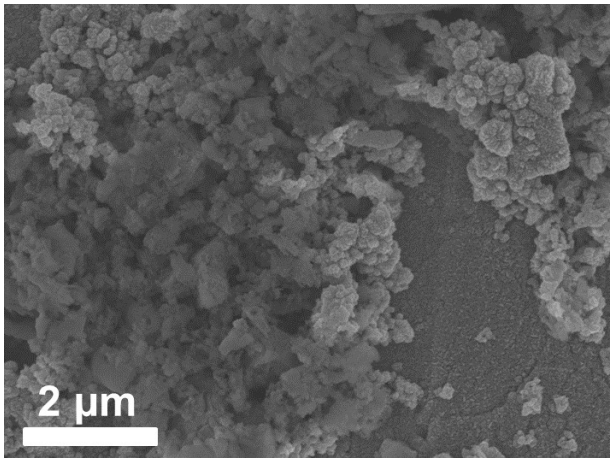


**Figure S9.** SEM image of the nanoporous A-Si materials.

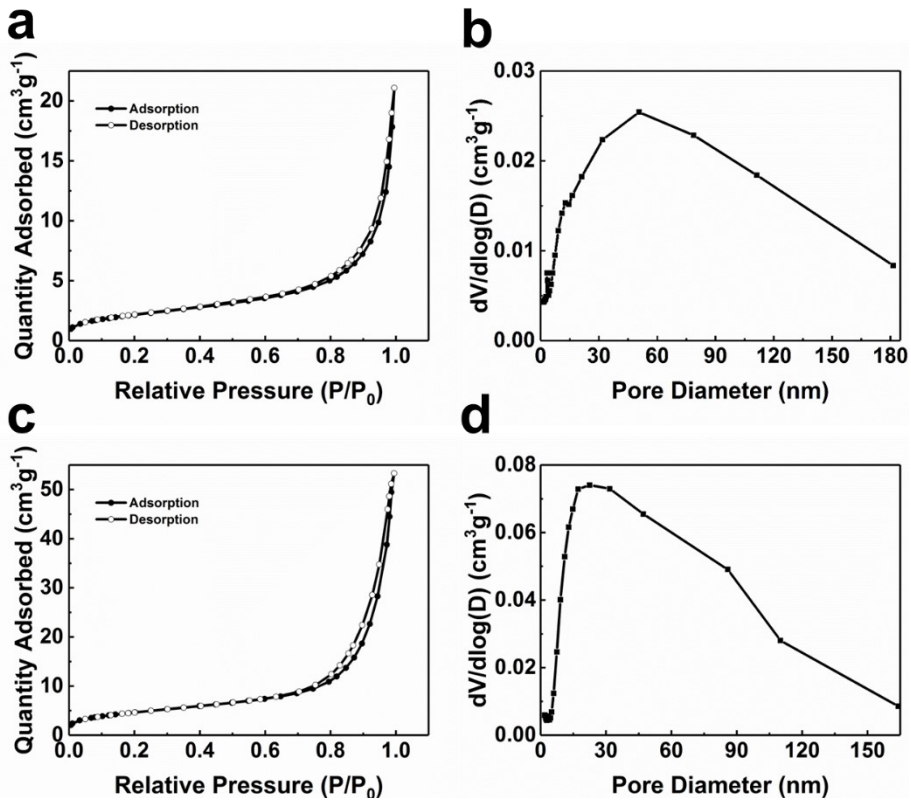


**Figure S10.** (a) $N_2$ adsorption-desorption isotherms and (b) the pore-size distribution calculated from the desorption branch of the nanoporous Z-Si materials. (c) $N_2$ adsorption-desorption isotherms and (d) the pore-size distribution calculated from the desorption branch of the nanoporous A-Si materials.

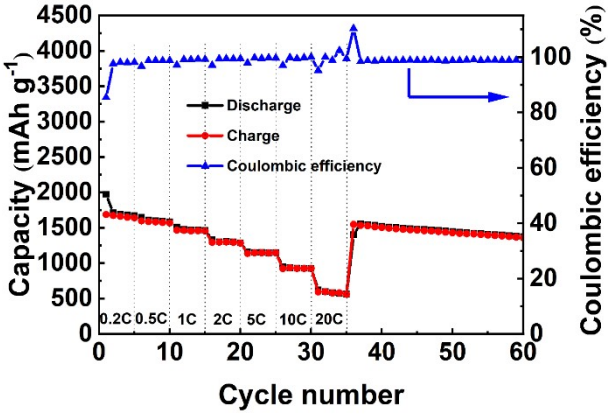


**Figure S11.** The rate capability of nanoporous Z-Si materials.

**Table S1.** Cyclability (discharge capacity) and the rate performance comparison of Z-Ge versus reported literature.

| Sample | Reversible capacity | Cycle number | Refs. |
|---|---|---|---|
| Porous Ge | 469 mAh $g^{-1}$ at 8 A $g^{-1}$ | 1800 | 1 |
| Ag/porous Ge | 493.2 mAh $g^{-1}$ at 3.2A $g^{-1}$ | 300 | 2 |
| Mesoporous Ge | 1217 mAh $g^{-1}$ at 1.28 A $g^{-1}$ | 400 | 3 |
| Nanoporous Ge | 1200 mAh $g^{-1}$ at 160 mA $g^{-1}$ | 200 | 4 |
| Marcoporous Ge | 911.2 mAh $g^{-1}$ at 150 mA $g^{-1}$ | 100 | 5 |
| Ge microcube | 682 mAh $g^{-1}$ at 1.6 A $g^{-1}$ | 500 | 6 |
| Ge nanotube arrays | 1004.5 mAh $g^{-1}$ at 320 mA $g^{-1}$ | 250 | 7 |
| Porous Ge nanowires | 888 mAh $g^{-1}$ at 800 mA $g^{-1}$ | 1100 | 8 |
| Z-Ge | 1002.8 mAh $g^{-1}$ at 3.2 A $g^{-1}$ | 700 | **This work** |

## References


1. K. Mishra, X.-C. Liu, F.-S. Ke and X.-D. Zhou, Porous germanium enabled high areal capacity anode for lithium-ion batteries, *Compos. B. Eng.*, 2019, **163**, 158-164.
2. J. Zhou, P. Huang, Q. Hao, L. Zhang, H. Liu, C. Xu and J. Yu, Ag nanoparticles anchored on nanoporous Ge skeleton as high-performance anode for lithium-ion batteries, *Chin. J. Chem*, 2021, **39**, 2881-2888.
3. N. Lin, T. Li, Y. Han, Q. Zhang, T. Xu and Y. Qian, Mesoporous hollow Ge microspheres prepared via molten-salt metallothermic reaction for high-performance Li-storage anode, *ACS Appl. Mater. Interfaces*, 2018, **10**, 8399-8404.
4. S. Liu, J. Feng, X. Bian, Y. Qian, J. Liu and H. Xu, Nanoporous germanium as

high-capacity lithium-ion battery anode, *Nano Energy*, 2015, **13**, 651-657.

5. S. Geier, R. Jung, K. Peters, H. A. Gasteiger, D. Fattakhova-Rohlfing and T. F. Fässler, A wet-chemical route for macroporous inverse opal Ge anodes for lithium ion batteries with high capacity retention, *Sustain. Energy Fuels.*, 2018, **2**, 85-90.

6. C. Zhang, Z. Lin, Z. Yang, D. Xiao, P. Hu, H. Xu, Y. Duan, S. Pang, L. Gu and G. Cui, Hierarchically designed germanium microcubes with high initial coulombic efficiency toward highly reversible lithium storage, *Chem. Mater.*, 2015, **27**, 2189-2194.

7. X. Liu, J. Hao, X. Liu, C. Chi, N. Li, F. Endres, Y. Zhang, Y. Li and J. Zhao, Preparation of Ge nanotube arrays from an ionic liquid for lithium ion battery anodes with improved cycling stability, *Chem. Comm.*, 2015, **51**, 2064-2067.

8. T. Kennedy, E. Mullane, H. Geaney, M. Osiak, C. O'Dwyer and K. M. Ryan, High-performance germanium nanowire-based lithium-ion battery anodes extending over 1000 cycles through in situ formation of a continuous porous network, *Nano Lett.*, 2014, **14**, 716-723.